Journal Name

ARTICLE

Different stabilities of liposomes containing saturated and unsaturated lipids toward the addition of cyclodextrins†

Received 00th January 20xx,
Accepted 00th January 20xx

DOI: 10.1039/x0xx00000x

www.rsc.org/

Atsushi Ikeda,* Rikushi Funada and Kouta Sugikawa

Liposomes composed of unsaturated lipids were more stable than those containing saturated lipids toward DMe-β-CDx, DMe-α-CDx and DMe-β-CDx. The Hill coefficient values (*n*) indicated that the saturated lipid•DMe-CDx complexes had stoichiometric ratios in the range of 1:3–1:4, while the unsaturated lipid•DMe-CDx complexes had ratios in the range of 1:1.5–1:3. That is, a *cis* alkene group in the unsaturated lipids prevented complexation with a second DMe-CDx in the direction toward each acyl chain. Furthermore, the liposomes composed of the unsaturated lipids were much slower to form precipitates upon the addition of α-CDx than those of the saturated lipids. To the best of our knowledge, this is the first example showing that CDxs interact with unsaturated lipids.

Introduction

Cyclodextrins (CDxs) and their derivatives have attracted considerable attention as drug carriers because their water solubility allows them to form inclusion complexes with hydrophobic drugs.[1,2] Recently, it has been reported that α-CDx and heptakis(2,6-di-*O*-methyl)-β-cyclodextrin (DMe-β-CDx) can include alkyl chains of lipids in their hydrophobic cavities, and the α-CDx•lipid complex forms a precipitate while the DMe-β-CDx•lipid complex dissolves in water.[3,4] The collapse of liposomes commonly occurs when these CDxs form complexes with lipids. The toxicity of CDxs is one of their most defining characteristics and is expected to be related to their interactions with lipids.[5–7] It is known that DMe-β-CDx has much higher toxicity than α-CDx.[8,9] We observed direct evidence for the interactions between DMe-β-CDx and saturated lipids, such as 1,2-dilauroyl-*sn*-glycero-3-phosphocholine (DLPC), 1,2-dimyristoyl-*sn*-glycero-3-phosphocholine (DMPC) and 1,2-dipalmitoyl-*sn*-glycero-3-phosphocholine (DPPC), and the DMe-β-CDx-mediated collapse of liposomes.[4] However, this study was not sufficient to allow us to conclude why DMe-β-CDx is highly toxic. The phospholipids of most biological membranes are characterised by a high percentage of *cis* unsaturated acyl chains. The biological importance of unsaturated fatty acids is believed to be related to the fact that their melting points are much lower than those of saturated fatty acids, with the result that membrane lipids containing *cis* unsaturated acyl chains tend to have lower temperatures of transition from the gel phase to the liquid crystalline phase. To the best of our knowledge, there are few studies on the complexation of CDxs and unsaturated lipids. Herein, we report that liposomes composed of unsaturated lipids are more stable than those of saturated lipids toward DMe-β-CDx, DMe-α-CDx and DMe-β-CDx.

Department of Applied Chemistry, Graduate School of Engineering, Hiroshima University 1-4-1 Kagamiyama, Higashi-Hiroshima 739-8527, Japan.

† Electronic Supplementary Information (ESI) available: UV-vis absorption and ^{1}H NMR spectra. See DOI: 10.1039/x0xx00000x

Results and discussion

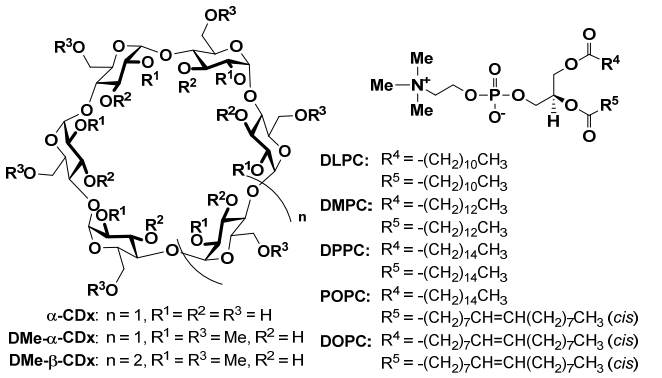

Evaluation of liposome stability toward the addition of DMe-β-CDx and DMe-α-CDx by UV-vis absorption measurements

Morphological changes in the liposomes were evaluated by UV-vis absorption spectroscopy based on variations in their light scattering intensity at 450 nm (A/A_0) in the presence of added DMe-β-CDx (Figs. 1 and S1). A decrease of the A/A_0 value was observed when the light scattering intensity decreased upon the collapse of liposomes after the addition of CDxs. This behaviour is similar to that observed for the collapse of liposomes after the addition of a suitable lysing agent (*e.g.*, ethanol) or a surfactant under aqueous conditions.[10,11]

As shown in Fig. 1 (green and red lines), the A/A_0 at 450 nm decreased after the addition of DMe-β-CDx to liposome solutions consisting of 1-palmitoyl-2-oleoyl-*sn*-glycero-3-phosphocholine (POPC) or 1,2-dioleoyl-*sn*-glycero-3-

phosphocholine (DOPC) with one and two *cis* alkene group(s). These results show that the stabilities of POPC with one *cis* alkene group and DOPC with two *cis* alkene groups are slightly higher than that of DPPC with saturated acyl chains of a similar chain length toward the addition of DMe-β-CDx. This indicates that the stabilities of the different liposomes toward DMe-β-CDx were of the order DOPC≈POPC>DPPC, which reflected the presence of *cis* alkene groups. That is, the stabilities of the lipid•DMe-β-CDx complexes decreased upon the introduction of *cis* alkene groups because the *cis* alkene groups prevent complexation with several DMe-β-CDx units in water. However, the small difference of the stabilities among these liposomes was contrary to our expectations. The labilities of the lipid•DMe-β-CDx complexes in the final state (Scheme 1B) and the liposomal stabilities in the initial state (Scheme 1C) are both believed to influence the overall liposomal stabilities. Although the liposomal stabilities cannot be directly estimated by the phase transition temperature (T_m) between the gel and liquid crystal-phases, the packing of the acyl chains is generally tighter so that the T_m is high. Because T_m values for DPPC, POPC and DOPC liposomes are 41, −2 and −17 °C, respectively, the liposomal stabilities are of the order DPPC>POPC>DOPC. The acyl side chains act to disturb the collapse of the liposome by complexation with DMe-β-CDx. Therefore, the effect of the labilities of the lipid•DMe-β-CDx complexes is expected to be offset by the liposomal stabilities, which will be examined in greater detail by using Hill plots.

There are a few differences in the nature of the interactions between unsaturated and saturated lipids in the corresponding DMe-β-CDx complexes. Here, one acyl chain would be too short to interact with three and four DMe-CDxs. Instead, one chain would be expected to interact with a maximum of two DMe-β-CDx units because the thickness of DMe-CDxs is approximately 8 Å and the lengths of the acyl chains with DPPC and DOPC having a completely anti-conformation are 17.8–20.2 Å. When two DMe-β-CDxs interact with one acyl chain of DOPC, one of the DMe-β-CDxs must pass through the *cis* alkene group (Scheme 1B). Therefore, we expect that the energy barrier is larger for DMe-α-CDx with a smaller cavity compared with DMe-β-CDx when a terminal methyl group of an acyl chain passes through each DMe-CDx cavity.

As shown in Figs. 1 (black and blue lines) and S2A, in the [DMe-β-CDx]/[DPPC] = 20 equiv. and [DMe-α-CDx]/[DPPC] = 35 equiv. cases, the minimum value of A/A_0 at 450 nm was observed, indicating that it is more difficult for DMe-α-CDx to collapse the DPPC liposome than DMe-β-CDx. These results are indirectly supported by the fact that DMe-β-CDx has been shown to be much more toxic than α-CDx. Although the minimum values of A/A_0 at 450 nm did not differ much between the DPPC and DOPC liposomes, the values of A/A_0 for DPPC immediately decreased compared with those for DOPC following the addition of a larger amount of DMe-α-CDx [Figs. 1 (blue and orange lines) and S2]. The difference between DPPC and DOPC toward DMe-α-CDx is larger than that toward DMe-β-CDx. These results clearly showed that the stability of the DOPC liposome was much higher than that of the DPPC liposome toward DMe-α-CDx.

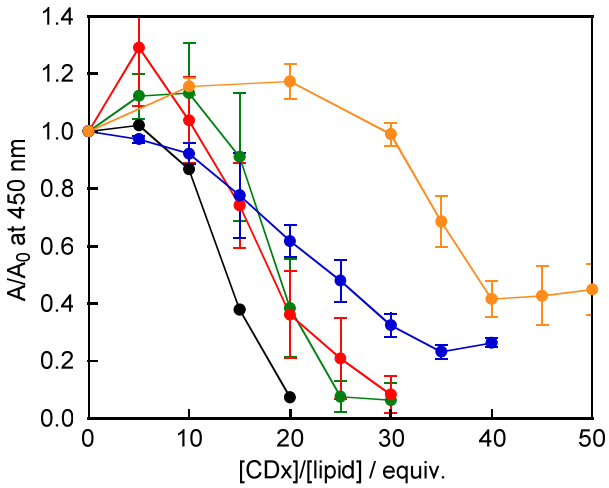

Fig. 1 Changes in the intensity (A/A_0) of the light scattering at 450 nm by UV-vis absorption spectroscopy for DPPC (black), POPC (green) and DOPC (red) liposomes both before and after the addition of DMe-β-CDx and for DPPC (blue) and DOPC (orange) liposomes both before and after the addition of DMe-α-CDx ([lipids] = 1.0 mM).

Visual examination of the liposome solutions

It is noteworthy that all of the changes described above could be observed by visual examination. As shown in Fig. 2A and E, aqueous solutions of the DPPC and DOPC liposomes had a similar turbidity to that of soapy water. The addition of DMe-β-CDx and DMe-α-CDx led to the clarification of these turbid solutions (Fig. 2B, D, G and I). The addition of DMe-β-CDx to a solution of DOPC liposomes ([DMe-β-CDx]/[lipid] = 20 equiv.) led to an increase in the clarity of the solution, with the DPPC solution becoming completely clear (Fig. 2B). In contrast, the addition of 30 equiv. of DMe-α-CDx to a turbid solution of DOPC liposomes had very little impact on the turbidity of the solution (Fig. 2H), with the solution only becoming clear following the addition of at least 40 equiv. of DMe-α-CDx (Fig. 2I). Therefore, these results were consistent with those observed for the changes in the light scattering as shown in Fig. 1.

Determination of the formation of lipid•DMe-β-CDx and DMe-α-CDx complexes by ^{1}H NMR analyses

The formation of the lipid•DMe-β-CDx complexes was confirmed by ^{1}H NMR analyses. In the absence of DMe-β-CDx, the ^{1}H NMR spectra of the POPC and DOPC liposomes did not contain any peaks that could be assigned to POPC and DOPC because of the extreme broadening of the signals resulting from the formation of the liposomes (Fig. 3A). However, several new peaks emerged in the range of 0.8–1.4 ppm after the addition of DMe-β-CDx and were assigned to the alkyl chains of individual POPC and DOPC molecules (Fig. 3C–E) because they were very similar to those observed in the ^{1}H NMR spectrum of the DPPC•DMe-β-CDx complex (Fig. 3B).[4] Therefore, these results suggested that the addition of DMe-β-CDx led to the collapse of the POPC and DOPC liposomes and that the isolation of the POPC and DOPC•DMe-β-CDx complexes in water was in agreement with the results reported above for the changes in the light scattering intensities (Fig. 1). The signals for free DMe-β-CDx and those of its complexes with POPC and DOPC did not

appear separately but merely broadened and shifted, indicating that the rate of the complexation–decomplexation exchange of DMe-β-CDx was occurring too quickly to be observed on the ^{1}H NMR time scale.

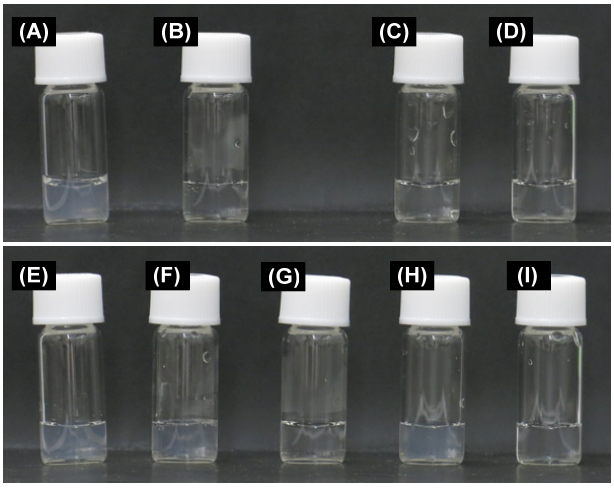

Fig. 2 Photographic images of aqueous solutions of the DPPC liposomes (A) before and after the addition of (B) 20 equiv. of DMe-β-CDx and (C) 20 equiv. and (D) 30 equiv. of DMe-α-CDx. Photographic images of the DOPC liposomes (E) before and after the addition of (F) 20 equiv. and (G) 30 equiv. of DMe-β-CDx and (H) 30 equiv. and (I) 40 equiv. of DMe-α-CDx ([lipids] = 1.0 mM).

The formation of the lipid•DMe-α-CDx complexes was also confirmed by ^{1}H NMR analyses (Fig. 3E and F). The ^{1}H NMR data indicated that DMe-α-CDx could form a pseudorotaxane conformation with the lipids in a manner similar to DMe-β-CDx. These results were not surprising because finely dispersed precipitates were observed immediately after mixing α-CDx with the DMPC and DPPC liposome solutions. Conversely, it suggested that the precipitates formed in the presence of α-CDx and saturated lipids are followed by the formation of the pseudorotaxane conformation. Although a small peak at 5.15 ppm is very similar to a H-1 proton peak of a [60]fullerene•γ-CDx complex, the same peak was observed for DMe-α-CDx in the absence of lipids. The commercial DMe-α-CDx consisted of a compound that had been methylated at 14 of the hydroxy groups on the 2- and 6-positions, as well as a compound that had been methylated at the 3-position as an impurity. It is known that it can be very difficult to separate and purify these types of compounds.[13] Therefore, the small peak at 5.3 ppm was assigned to the H-1 proton of the impurity methylated at the 3-position. Consequently, the signals for free DMe-β-CDx and those of its complexes with DPPC and DOPC did not appear separately but merely broadened and shifted compared with the original signals, which indicated that the rate of the complexation-decomplexation exchange of DMe-α-CDx was occurring too quickly to be observed on the ^{1}H NMR time scale.

Evaluation of the allosteric effects using Hill plots

The proportion of isolated lipid relative to the total lipid ($[\text{lipid}]_c/[\text{lipid}]_0 = y$; $[\text{lipid}]_c$: concentration of lipid in the

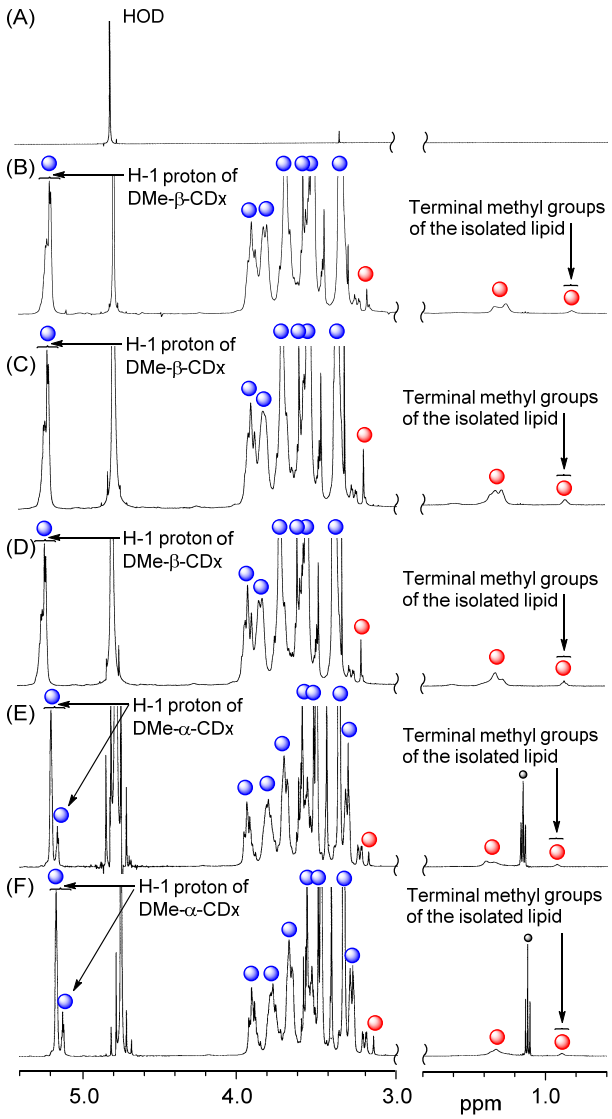

Fig. 3 Partial ^{1}H NMR spectra of (A) POPC liposome, (B) DPPC•DMe-β-CDx complex, (C) POPC•DMe-β-CDx complex, (D) DOPC•DMe-β-CDx complex, (E) DPPC•DMe-α-CDx complex and (F) DOPC•DMe-α-CDx complex {[lipid] = 1.0 mM, [DMe-CDx]/[lipid] = 20 equiv., blue circles: DMe-CDx, red circles: lipid, black circles: ethanol contained in DMe-α-CDx}[12]. D_2O, 23 °C, 400 MHz.

lipid•DMe-β-CDx complex, $[\text{lipid}]_0$: total concentration of lipid) can be readily estimated from the ratio of the peak intensities of the isolated lipid at 1.3 ppm and DMe-β-CDx molecules at 5.2 ppm in the ^{1}H NMR spectrum of a lipid•DMe-β-CDx complex (Figs. S3 and S4). We determined the complexation rate (y) of the DOPC liposome and compared it with the previous result obtained for DPPC liposomes.[4] A plot of the proportion of isolated DOPC *versus* [DMe-β-CDx] gave a sigmoidal curve,[14–22] which indicated that the binding of DMe-β-CDx to DOPC occurred according to a well-defined cooperative phenomenon (Fig. 4A red circles). This result was similar to that of the DPPC•DMe-β-CDx complex. The DMe-β-CDx-binding profile of this complex was analysed using the Hill equation: $\log [y/(1-y)] = n \log [\text{DMe-β-CDx}] - \log K$, where K and n are the association constant and Hill coefficients, respectively, and $y = K/([\text{guest}] - n - K)$.[23,24] In the range of [DMe-β-CDx] < 5.0 mM (5.0 equiv. for

lipids), the peak of the isolated DOPC molecules was too small to allow for the accurate calculation of *y*. From the slope and the intercept of the linear plot, we obtained *n* and log *K* values for the DOPC•DMe-β-CDx complex (Table 1), respectively. The fact that the Hill coefficient was close to 3 indicated that the complexes allowed for the highly cooperative binding of three DMe-β-CDxs. As mentioned above, the maximum amount of DMe-CDxs that can include one acyl chain is two because of the thickness of the DMe-CDxs and the length of the acyl chain of DOPC. Because the Hill coefficient for the DOPC•DMe-β-CDx complex (n = 2.9) was lower than that of the saturated DPPC•DMe-β-CDx complexes (n = 3.6), these results suggest that the *cis* alkene groups of DOPC prevent complexation with the second DMe-β-CDx in the direction of the acyl chain in water (Scheme 1B). The DOPC•DMe-β-CDx complex was evaluated by isothermal titration calorimetry (ITC) in water (Fig. S5). However, it was difficult to determine thermodynamic parameters because there are unknown six parameters (K_1, ΔH_1, K_2, ΔH_2, K_3 and ΔH_3).[25]

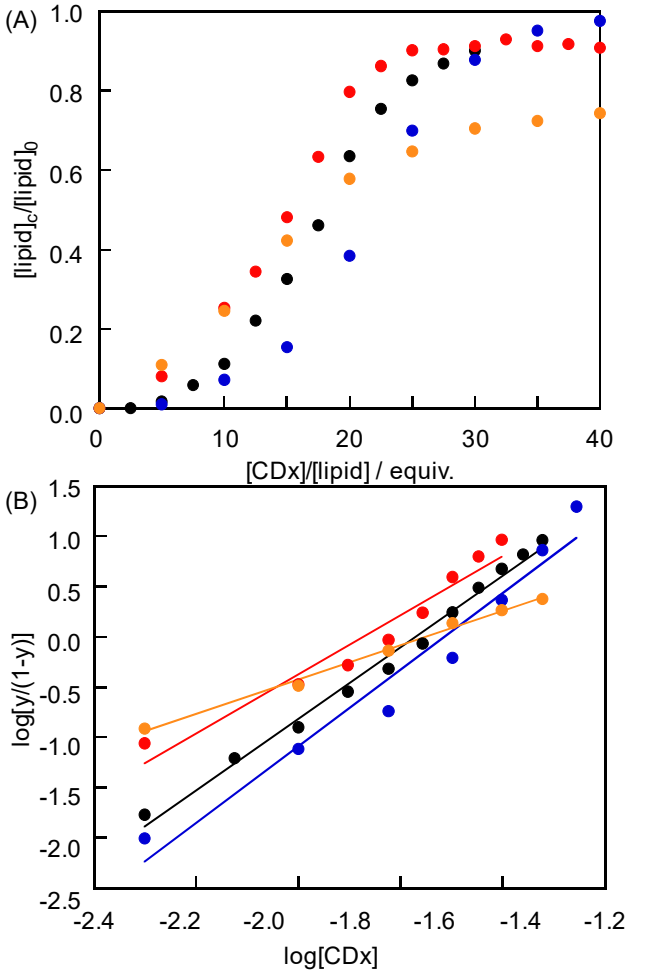

Fig. 4 (A) Plot of $[lipid]_c/[lipid]_0$ (=*y*) *versus* [CDx] {$[lipid]_c$: concentration of lipid in the lipid• CDx complex, $[lipid]_0$: total concentration of lipid (1.0 mM)} and (B) plot of log [*y*/(1–*y*)] *versus* log [CDx] for the DPPC•DMe-β-CDx complex (black), DOPC•DMe-β-CDx complex (red), DPPC•DMe-α-CDx complex (blue) and DOPC•DMe-α-CDx complex (orange).

The log *K* value for the DOPC•DMe-β-CDx complex was calculated to be 5.3 (ΔG = –30.5 kJ•mol^{-1}) (correlation coefficient 0.98) (Table 1). However, the log *K* value cannot be compared with that for the DPPC•DMe-β-CDx complex (log *K* = 6.3; ΔG = –36.1 kJ•mol^{-1}) because these association constants (*K*) have different dimentions because of the different Hill coefficients. In contrast, because the Hill coefficient for DOPC was very similar to that for DLPC (n = 3.0), the log *K* value for the DOPC•DMe-β-CDx complex can be compared with that for the DLPC•DMe-β-CDx complex (log *K* = 7.3; ΔG = –41.6 kJ•mol^{-1}). The results show that DOPC with two *cis* alkene groups binds more weakly to a few DMe-β-CDxs in water than DLPC with its shorter acyl chains. This may be explained by the examining the labilities of the DOPC•DMe-β-CDx complex in the final state. The resulting 1:3 DOPC•DMe-β-CDx complex is less water soluble than the 1:3 DLPC•DMe-β-CDx complex because the acyl chain length of DOPC is longer than that of DLPC. That is, in the 1:3 DOPC•DMe-β-CDx complex, the hydrophobic acyl chain of DOPC cannot be completely encapsulated by three DMe-β-CDxs.

Table 1 Binding parameters obtained from the Hill plot.

Complex	log K^a	n^a	R^b	Ref.
DLPC•DMe-β-CDx complex	7.3	3.0	0.98	4
DPPC•DMe-β-CDx complex	6.3	3.6	0.99	4
DOPC•DMe-β-CDx complex	5.5	2.9	0.97	This work
DPPC•DMe-α-CDx complex	6.5	3.8	0.98	This work
DOPC•DMe-α-CDx complex	3.0	1.7	0.99	This work

[a]Association constant and Hill coefficient obtained from Hill equation (see text).
[b]Correlation coefficient of Hill plot.

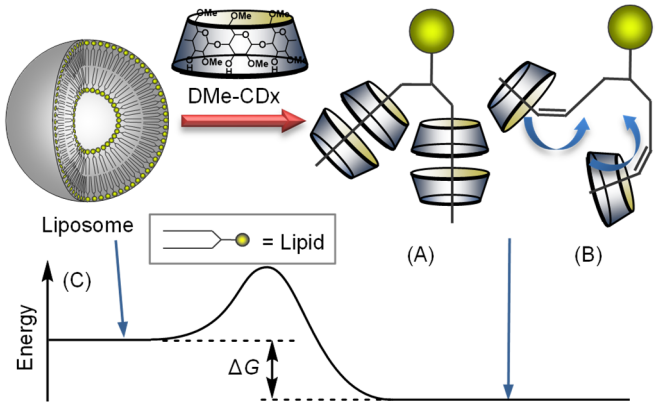

Scheme 1. Schematic illustration of (A) the DPPC•DMe-CDx and (B) the DOPC•DMe-CDx complexes and (C) energy diagram

The *y* values can be also estimated from the ratio of the peak intensities of the isolated lipid at 0.9 ppm and DMe-α-CDx molecules at 5.2 ppm in the ^{1}H NMR spectra of a lipid•DMe-α-CDx complex because the peak at 1.25 ppm overlap with a peak of ethanol at 1.1 ppm. We obtained a log *K* value of 6.5 (ΔG = –37.4 kJ•mol^{-1}) for the DPPC•DMe-α-CDx complex (correlation coefficient 0.98), together with an n value of 3.8 (Figs. 4B and S6 and Table 1). The Hill coefficient for the DPPC•DMe-α-CDx

complex was very similar to that for the DPPC•DMe-β-CDx complex (n = 3.6). The values of n are believed to be similar because although DMe-α-CDx and DMe-β-CDx have different cavity sizes but the same width, a DPPC alkyl chain is equally encapsulated by these two CDxs. In contrast, the Hill coefficient for the DOPC•DMe-α-CDx complex (n = 1.7) was much lower than that for the DOPC•DMe-β-CDx complex (n = 2.9) (Figs. 4B and S7 and Table 1). This is indicates that the corresponding DOPC•DMe-α-CDx complex was primarily formed in a 1:2 molar ratio. Thus, as expected, it was difficult for the DMe-α-CDx unit with a smaller cavity to encapsulate the *cis* alkene groups (Scheme 1B).

Precipitation of lipids in the presence of added α-CDx

Csempesz *et al*. reported that a finely dispersed precipitate was observed immediately after mixing α-CDx with a DPPC liposome solution.[3] It is difficult to directly analyse the nature of the interactions between DPPC and α-CDx because the resulting precipitate is insoluble in water. Therefore, we investigated the concentrations of residual DPPC and α-CDx in water. After the addition of α-CDx ([DPPC]/[α-CDx] = 10 equiv.), the DPPC concentration in water was calculated by measuring phosphatidylcholine through an enzymatic method (LabAssay™ Phospholipid, Wako, Osaka, Japan). Figure 5 shows that DPPC precipitated rapidly. To determine the stoichiometry of the precipitates, we measured the concentration of residual α-CDx in water by ^{1}H NMR because the DPPC•α-CDx complex could not be redissolved in DMSO-d_6. Furthermore, the concentration of residual α-CDx in water was evaluated based on the ratio of the ^{1}H NMR peak integrals for the signals of α-CDx and DMSO after the addition of a known amount of DMSO (0.05 mM). After 24 h, all DPPC precipitated, and we calculated that the concentration of residual α-CDx in water was 6.0 mM. This indicates that the precipitated DPPC•α-CDx complex was formed in an approximate 1:4.0 ratio.

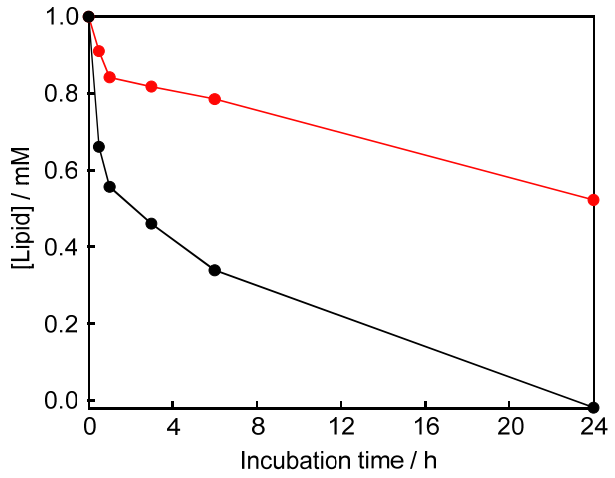

Fig. 5 Dependence of the incubation time on the concentration of lipids in the DPPC•α-CDx (black) and DOPC•α-CDx (red) mixture in water {[lipid] = 1.0 mM, [α-CDx]/[lipid] = 10 equiv.}.

After mixing with α-CDx, the DOPC liposome solution became slowly turbid. This observation is consistent with the result in Fig. 5 (red), which shows that DOPC precipitated slower than DPPC. Therefore, we measured the ^{1}H NMR spectrum of DOPC immediately after the addition of α-CDx ([DPPC]/[α-CDx] = 10 equiv.). New peaks emerged in the range of 0.8–1.4 ppm and were assigned to the acyl chains of DOPC in the DOPC•α-CDx complex (Fig. 6 red circles). These peaks were very small but were very similar to those in the spectra of the DOPC•DMe-β-CDx and DOPC•DMe-α-CDx complexes (Figs. 3 and 6). This suggests that (i) first, the DOPC•α-CDx complex was formed and then precipitated, and (ii) the rate of formation of the DOPC•α-CDx complex is much slower than the rate of formation of the DOPC•DMe-α-CDx complex because α-CDx has a more rigid cavity than DMe-α-CDx. Although the reason for the precipitation of the lipid•α-CDx complexes is not clear, the complexation of the lipid and α-CDx expands the α-CDx cavity and modifies the hydrogen bonding of α-CDx from intramolecular to intermolecular, similar to what was observed for the [60]fullerene•calix[8]arene complex.[26–29] In contrast, no peaks emerged in the range of 0.8–1.4 ppm immediately after the mixing of the DPPC and α-CDx solutions (Fig. S8). This suggests that after the formation of the complex, the DPPC•α-CDx complex precipitates rapidly. The concentration of residual α-CDx in water was calculated in the DOPC•α-CDx complex in a similar manner as the DPPC•α-CDx complex. However, the ^{1}H NMR spectrum was obtained after 5 days when all the DOPC was precipitated. The concentration of residual α-CDx was calculated to be 6.9 mM. Because the initial concentrations of α-CDx and DOPC were 10.0 and 1.0 mM, respectively, the precipitated DOPC•α-CDx complex was formed in an approximate 1:3.1 ratio. In the precipitates, the amount of α-CDx in the DOPC•α-CDx complex was smaller than that in the DPPC•α-CDx complex. Two possibilities may explain the slow precipitation of the DOPC complex, as follows: (a) the rate of formation of the 1:3 DOPC•α-CDx complex is much slower than that for the 1:4 DPPC•α-CDx complex because of the steric hindrance of the *cis* alkene groups in DOPC; and (b) the rate of formation of the intramolecular hydrogen bonding of α-CDx in the 1:3 DOPC•α-CDx complex is much slower than that in the 1:4 DPPC•α-CDx complex because of small amounts of α-CDx in the former complex. It is very difficult to determine the mechanism, but Figs. 6 and S8 support that explanation (b) may be correct because the DOPC•α-CDx complex was observed in water but the DPPC•α-CDx complex was not.

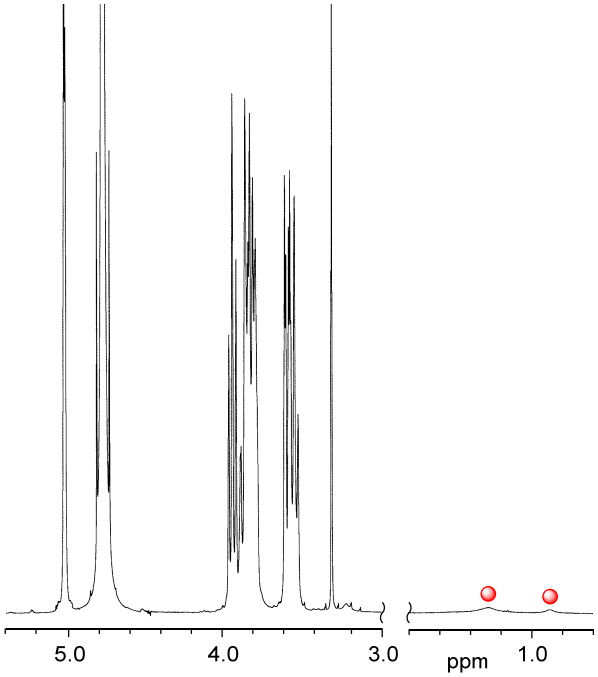

Fig. 6 Partial ^{1}H NMR spectrum of the DOPC•α-CDx mixture immediately after mixing {[DOPC] = 1.0 mM, [α-CDx]/[DOPC] = 10 equiv., red circles: lipid }. D_2O, 23 °C, 400 MHz.

Selectivity of saturated and unsaturated lipids toward the addition of α-CDx

As mentioned above, DOPC complexes precipitated slower than DPPC complexes upon the addition of α-CDx. In the presence of liposomes consisting of saturated and unsaturated lipids, the selectivity of α-CDx was investigated in the precipitates. To determine the stoichiometry of saturated and unsaturated lipids in the precipitates, we measured the concentration of residual saturated and unsaturated lipids in water by the ^{1}H NMR spectra after 6 h. The results were summarised in Fig. 7. As shown in Fig. 5, approximately 66 and 21% DPPC and DOPC, respectively, precipitated after 6 h. In contrast, in Fig. 7, approximately 66 and 38 % DPPC and DOPC, respectively, precipitated. The content of DOPC (38%) in the precipitate in the presence of DPPC and DOPC liposomes is higher than that (21%) in the DOPC liposome alone. This suggests that the DPPC•DMe-α-CDx complex participated in precipitating the DOPC•DMe-α-CDx complex. Although the difference in the amounts between DPPC and DOPC was smaller than predicted by the results shown in Fig. 5, the amount of DPPC was higher than that of DOPC in the precipitate.

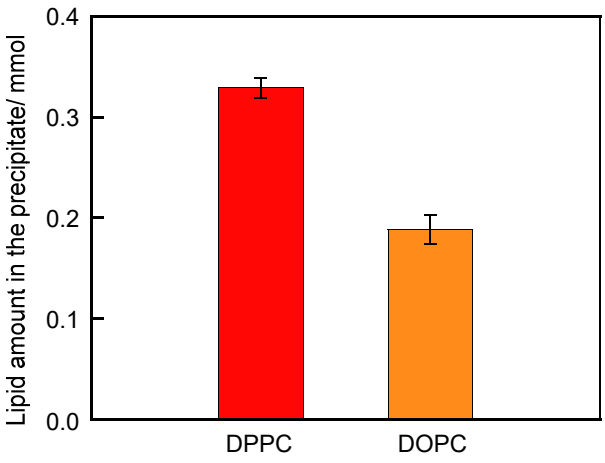

Fig. 7 Amount of DPPC (red bar) and DOPC (orange bar) in the precipitate 6 h after addition of α-CDx (1.0 mL, [DPPC] = [DOPC] = 0.50 mM, [α-CDx] = 10 mM).

Experimental

Materials

DMe-β-CDx was purchased from Sigma-Aldrich Chemical Co., Inc. (St. Louis, MO, USA). DMe-α-CDx and α-CDx were obtained commercially from Wako Pure Chemical Ind. Ltd. (Osaka, Japan). 1,2-Dipalmitoyl-*sn*-glycero-3-phosphocholine (DPPC), 1-palmitoyl-2-oleoyl-*sn*-glycero-3-phosphocholine (POPC) and 1,2-dioleoyl-*sn*-glycero-3-phosphocholine (DOPC) were obtained from Avanti Polar Lipids, Inc. (Alabaster, USA).

Preparation of liposomes

Solutions of DPPC, POPC and DOPC (1.44×10^{-5} mol) in chloroform (1 mL) were dried using a rotary evaporator at 40 °C. Water (4.0 mL) was added to the solution, and the resulting mixture was shaken on a vortex mixer for 5 min. To change from multilamellar to unilamellar vesicles and obtain a narrow size distribution, the solution was subjected to a freeze-thaw cycle (three times) and extruded 11 times (LiposoFast-Basic; Avestin Inc., Ottawa, Canada) with two stacked polycarbonate membranes, pore size 50 nm. The resulting solution was diluted with water to a final concentration of 2.0 mM lipids.

Mixing of liposomes with the cyclodextrins

An aqueous solution of CDx (DMe-β-CDx, DMe-α-CDx or α-CDx) (1.0 mL, 0–40.0 mM) was mixed with an aqueous solution of liposomes (1.0 mL, [lipid] = 2.0 mM) at room temperature in a 5 mL glass vial. The [CDx]/[lipid] ratio was varied from 5.0 to 30 for DPPC, from 5.0 to 35 for POPC and from 5.0 to 50 for DOPC.

Mixing of the DPPC and DOPC liposomes with the α-cyclodextrin

Aqueous solutions of DPPC liposomes and DOPC liposomes (each 250 μL, 2.0 mM) were mixed at room temperature in a 5 mL glass vial. An aqueous solution of α-CDx (500 μL, 20.0 mM) was added in the mixture (1.0 mL, [DPPC] = [DOPC] = 0.50 mM, [α-CDx] = 10.0 mM). After incubation for 6 h at room temperature and centrifugation, the supernatant solution (500

μL) was lyophilized. The resulting white solid was dissolved in DMSO-d_6 containing 1 mM chloroform and its ^{1}H NMR spectrum was obtained. Each lipid concentration in the supernatant solution was calculated using the peak intensities of DPPC and DOPC compared with that of chloroform.

Light scattering measurement by UV-vis absorption spectroscopy

The UV-vis spectra were recorded using a UV-3600PC spectrophotometer (Shimadzu Corp., Kyoto, Japan). All of the experiments were performed at 25 °C using a 1 cm cell.

^{1}H NMR spectroscopy

^{1}H NMR spectra were recorded on a Varian 400-NMR (400 MHz) (Varian Associates, Inc., Palo Alto, CA, USA).

Microcalorimetric measurements

An isothermal calorimetry (ITC) instrument (MicroCal iTC200, Malvern Instruments Ltd., Worcestershire, UK) was used for a microcalorimetric experiment. A constant volume (2 μL/injection, 100 mM) of DMe-β-CDx was injected into the reaction cell (200 μL, [DOPC] = 0.5 mM) charged with a DOPC liposome solution in water. The heat of dilution of when the DMe-β-CDx solution was added to the aqueous solution in the absence of DOPC liposomes was determined in the same number of injections and concentration of DMe-β-CDx as used in the titration experiments. The dilution enthalpies determined in the control experiment were subtracted from the enthalpies measured in the titration experiments.

Determination of phospholipid concentrations

After the addition of α-CDx, the DPPC and DOPC concentrations in water were assayed with the LabAssay Phospholipid kit LabAssay™ Phospholipid, Wako, Osaka, Japan). Preparation of reagents and analysis of all parameters were carried out according to the manufacturer's instructions.

Conclusions

The results of the current study showed that liposomes collapse following the addition of a significant excess of not only DMe-β-CDx but also DMe-α-CDx through allosteric interactions. However, the interactions between DMe-α-CDx and lipids were weaker than those between DMe-β-CDx and the same size lipids, suggesting that the lipid content of the cell membrane plays a role in the observed differences in the cytotoxicity of DMe-α-CDx compared with that of DMe-β-CDx. Furthermore, the liposomal collapse was inhibited when the liposomes contained unsaturated lipids. It was concluded that the presence of the DOPC *cis* alkene groups prevented complexation with a second DMe-CDx in the direction toward each acyl chain based on the following two results: (i) It was more difficult to collapse the DOPC liposome upon addition of DMe-α-CDx with its smaller cavity than DMe-β-CDx and (ii) the Hill coefficient for the DOPC•DMe-α-CDx complex (n = 1.7) was much smaller than that for the DOPC•DMe-β-CDx complex (n = 2.9). That is, when the second unit of DMe-CDx is directed toward one acyl chain, particularly DMe-α-CDx, it is difficult to encapsulate the *cis* alkene groups. Furthermore, the rate of formation of the DOPC•α-CDx complex is much slower than the rate of formation of the DPPC•α-CDx complex. These observations suggest that the cytotoxicity of DMe-β-CDx, DMe-α-CDx and α-CDx may be related to the ratio of saturated to unsaturated lipids in the cellular membranes.

Acknowledgements

This work was supported by the Japanese Society for the Promotion of Science (JSPS) KAKENHI a Grant-in-Aid for Scientific Research (B) (Grant No. 25288037 and No. 16H04133) and a Grant-in-Aid for Challenging Exploratory Research (Grant No. 16K13982). The authors would like to express their deepest gratitude to Prof. Takashi Morii and Dr. Eiji Nakata, Institute of Advanced Energy, Kyoto University for their kind permission to use the iTC200 and providing technical assistance with the ITC measurements.

Notes and references

1 J. Szejtli, *Chem. Rev*. **1998**, *98*, 1743–1753.
2 G. Crini, *Chem. Rev*. **2014**, *114*, 10940–10975
3 I. Puskás and F. Csempesz, *Colloids Surf. B,* 2007, **58**, 218–224.
4 A. Ikeda, N. Iwata, S. Hino, T. Mae, Y. Tsuchiya, K. Sugikawa, T. Hirao, T. Haino, K. Ohara and K. Yamaguchi, *RSC Adv*., 2015, **5**, 77746−77754.
5 J. Szejtli, T. Cserhati and M. Szogyi, *Carbohydr. Polym*., 1986, **6**, 35–49.
6 J. Nishijo and H. Mizuno, *Chem. Pharm. Bull*., 1998, **46**, 120–124.
7 G. Piel, M. Piette, V. Barillaro, D. Castagne, B. Evrard and L. Delattre, *Int. J. Pharm*., 2007, **338**, 35–42.
8 F. W. H. M. Merkus, N. G. M. Schipper and J. C. Verhoef, *J. Control. Rel*., 1996, **41**, 69–75.
9 S. Gould and R. Scott, *Food Chem. Toxicol*., 2005, **43**, 1451–1459.
10 S. M. K. Davidson and S. L. Regen, *Chem. Rev.*, 1997, **97**, 1269–1279 and references therein.
11 A. Mueller and D. F. O'Brien, *Chem. Rev.*, 2002, **102**, 727–757 and references therein.
12 Ethanol was not removed from the solid state of DMe-α-CDx under vacuum for 12 h at 80 °C.
13 C. M. Spencer, J. F. Stoddart and R. Zarzycki, *J. Chem. Soc., Perkin Trans. 2*, 1987, 1323–1335.
14 S. Shinkai, A. Sugasaki, M. Ikeda and M. Takeuchi, *Acc. Chem. Res.*, 2001, **34**, 494–503.
15 M. Takeuchi, A. Sugasaki, M. Ikeda and S. Shinkai, *Acc. Chem. Res*., 2001, **34**, 865–873.
16 M. Takeuchi, T. Imada and S. Shinkai, *Angew. Chem., Int. Ed*., 1998, **37**, 2096–2099.
17 A. Sugasaki, M. Ikeda, M. Takeuchi and S. Shinkai, *Angew. Chem., Int. Ed.*, 2000, **39**, 3839–3842.
18 A. Sugasaki, K. Sugiyasu, M. Ikeda, M. Takeuchi and S. Shinkai, *J. Am. Chem. Soc.*, 2001, **123**, 10239–10244.
19 O. Hirata, M. Takeuchi and S. Shinkai, *Chem. Commun*., 2005, 3805–3807.
20 T. Ikeda, O. Hirata, M. Takeuchi and S. Shinkai, *J. Am. Chem. Soc.*, 2006, **128**, 16008–16009.
21 M. Ikeda, Y. Kubo, K. Yamashita, T. Ikeda, M. Takeuchi and S. Shinkai, *Eur. J. Org. Chem*., 2007, **2007**, 1883–1886.

22 R. Wakabayashi, T. Ikeda, Y. Kubo, S. Shinkai and M. Takeuchi, *Angew. Chem., Int. Ed*., 2009, **48**, 6667–6670.
23 B. Perlmutter-Hayman, *Acc. Chem. Res.*, 1986, **19**, 90–96.
24 K. A. Connors, *Binding Constants*, Wiley, New York, 1987.
25 M. Rekharsky and Y. Inoue, *J. Am. Chem. Soc.*, 2000, **122**, 10949–10955.
26 J. L. Atwood, G. A. Koutsantonis and C. L. Raston, *Nature*, 1994, **368**, 229–231.
27 T. Suzuki, K. Nakashima and S. Shinkai, *Chem. Lett*., 1994, 699–702.
28 T. Suzuki, K.; Nakashima and S. Shinkai, *Tetrahedron Lett.*, 1995, **36**, 249–252.
29 C. L. Raston, J. L. Atwood, P. J. Nichols and I. B. N. Sudria, *Chem. Commun*., 1996, 2615–2616.

